ORIGINAL PAPER

Investigations on the Thermocapillary Migration of Liquid Lubricants at Different Interfaces

Zhejun Chong[1] · Qingwen Dai[1] · Wei Huang[1] · Xiaolei Wang[1]

Abstract
Thermocapillary migration describes an interfacial phenomenon that liquids can spontaneously move from the warm to the cold regions on nonuniformly heated solids. However, it is unknown how liquids react at various interfaces subjected to a thermal gradient. In this study, migration of liquid lubricants at the free surface, the plate/plate interface, and the sphere/plate interface is investigated. The results show that liquid lubricants can easily migrate at the free surface and the plate/plate interface, and the velocity at the free surface is much faster than that at the plate/plate interface. Interestingly, liquid lubricants maintain at the sphere/plate interface for a long time, and a continuous loss of a thin liquid film is observed at the cold side on the plate. The factors that influence the migration performances at these interfaces are examined. Numerical simulations are performed to reveal the mechanism and differences among them.

Graphical Abstract
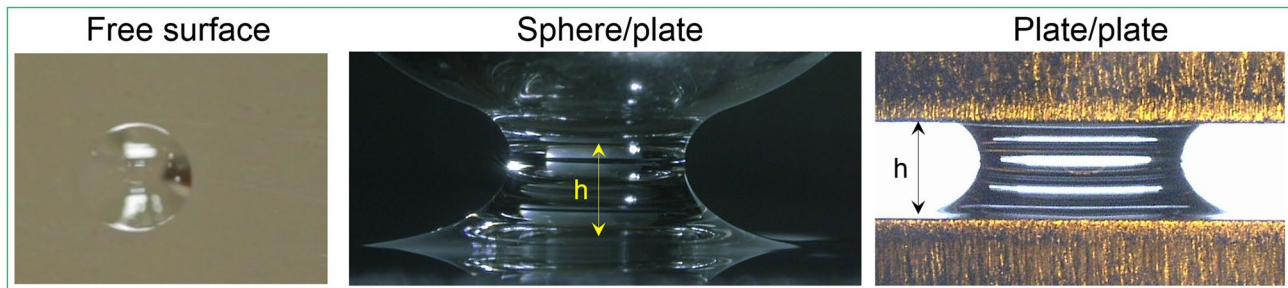
Zhejun Chong and Qingwen Dai have contributed equally to this work and should be considered as co-first authors.

This article is part of the Topical Collection on International Nanotribology Forum: Chiang Rai 2020.

Electronic supplementary material The online version of this article (https://doi.org/10.1007/s11249-020-01299-5) contains supplementary material, which is available to authorized users.

✉ Qingwen Dai
  daiqingwen@nuaa.edu.cn

1 National Key Laboratory of Science and Technology On Helicopter Transmission, Nanjing University of Aeronautics & Astronautics, Nanjing 210016, China

Abbreviations

A_r, A_{at}	Relative and absolute tolerances
Ca	Capillary number
C_p	Specific heat capacity at constant pressure
E_k	Error estimate for the degree of freedom k
F	Volume force vector
H, W	Eight and width of the computational domain
M	Number of physical fields
Ma	Marangoni number
N_j	Number of degrees of freedom in field j
P	Pressure
Q	Heat source
R	Strain-rate tensor
$S(x)$	Gas/liquid interface
T	Temperature

| T_{ref}	Reference ambient temperature
T_{Δ}	Thermal gradient
T_0	Reference temperature of liquid
U	Velocity vector
V	Solution vector
d	Mean liquid thickness
l, g	Liquid and gas
h	Gap between the plate/plate or sphere/plate interfaces
k	Fluid thermal conductivity
q	Heat flux vector
x, z	Horizontal and vertical coordinates
z_{max}	Maximum value of z at a specific x
Φ	Level set function
Ω_1	Gas subdomain
Ω_2	Liquid subdomain
a	Fluid thermal diffusivity
θ	Contact angle
β	Slip length
ε	Interface thickness
γ	Surface tension of liquid
γ_T	Surface tension coefficient of liquid
μ	Dynamic viscosity
κ	Re-initialization parameter
ρ	Fluid density
τ	Viscous stress tensor

1 Introduction

The Marangoni flow describes an interfacial phenomenon of mass transfer induced by surface tension gradients along the interface of two phases, particularly, the liquid/gas interface [1–3]. Variations in the solute or surfactant concentrations of liquids could both alter the surface tension, yielding a locomotion. In the case of temperature dependence, this phenomenon is widely known as thermocapillary migration (or convection). It is encountered in many applications such as hard disks, inkjet printers, heat transfer and condensations, especially in tribo-systems where thermal gradients are presented due to the proximity of an external heat source or an internal frictional heat, lubricant migration inevitably occurs.

On the one hand, a slight migration helps lubricants wetting the rubbing surfaces, enhancing the tribological performances. On the other, an excessive migration can result in a starved or dry lubrication condition. To slow or obstruct this thermal flow, numerous investigations concerning the migration at free surfaces have been carried out over the past decades. Experimentally, it is proven that coating low-surface energy materials [4] or constructing steep edges around migration regions [5], roughening surfaces via grinding [6] or shot-blasted processes [7], fabricating microstructures pattern [8] or wettability gradient [9–11] on migration regions are all feasible anti-migration strategies. Theoretically, after the lubrication approximate theory [12, 13] was introduced to simplify the migration model at free surfaces, slip boundary condition [14], contact angle hysteresis effect [15], and viscosity-temperature dependence [16] were all successfully involved in enhancing the prediction results. These studies have made important contributions to understanding the migration mechanism at free surfaces.

Regarding the attentions to practical applications, it is apparent that compared with the free surfaces, liquids at the interfaces of sphere/plate or plate/plate are more closely relevant to the work conditions of tribo-components, such as rolling or sliding bearings. This raises an essential question that, when encountered with thermal gradients, what will happen to liquid lubricants at the interfaces of sphere/plate or plate/plate? Will the migration occurs there? If it does, what are the internal similarities and differences among them? Examination of the existing literatures indicates that knowledge on these aspects is currently lacking. Revealing

Fig. 1 Schematic diagram of the constructed free surface, plate/plate and sphere/plate interfaces for migration tests
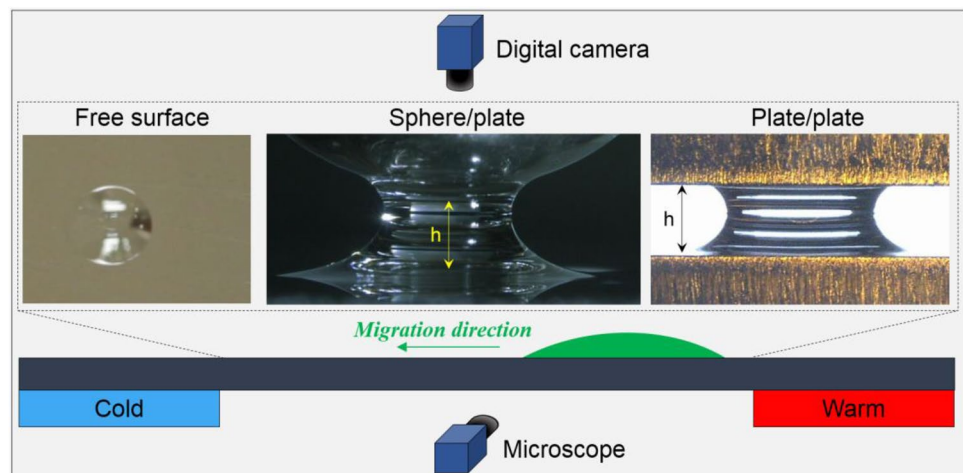
the migration mechanism at different interfaces and the corresponding influence factors can guide the design of modern tribological components that are exposed to thermal gradients.

In the light of the above facts, we experimentally investigate the thermocapillary migration of liquid lubricants at the free surface, the plate/plate interface, and the sphere/plate interface. The influences of thermal gradients, gap between the interfaces on the migration performances are discussed. Numerical simulations are performed to reveal the migration mechanism and the differences among them.

2 Experiments

Figure 1 shows the schematic diagram of experimental apparatus designed in this study. The sphere specimen was made of bearing steel (GCr15) with a diameter of 10 mm. The plate specimens were made of 304 stainless steel with dimensions of $60 \times 25 \times 2$ mm and an average surface roughness of ~0.05 μm.

Ends of one plate are fixed on two temperature controllable components (Misumi, Japan), of which one is a Peltier cooler and the other is a ceramic heater. By controlling their temperatures simultaneously, thermal gradients can be generated at the free surface. To construct a sphere/plate interface, a sphere is fixed to an aluminum fixture and held by a precision mobile platform for adjusting the gap (h) between the sphere/plate. Since the sphere is not in direct contact with the plate, and the heat conductivity of the aluminum fixture (~230 W/mK) is much higher than that of the oil (~0.1 W/mK) and the air (~0.02 W/mK), the temperature of sphere can maintain at ambient temperature (~20 °C). To construct a plate/plate interface, ends of another plate are directly supported by two square copper blocks (25 mm in width, varying thickness) and fixed right above the heated plate. The gap (h) between the plate/plate is equal to the thickness of the copper blocks. Since the copper blocks have an excellent heat conductivity and the maximum thickness is just 1.5 mm (Table 1), it is reasonable to believe that the temperature of the ends of the upper plate is same as the bottom one. The constructed three interfaces can be clearly seen in the insert graphs.

Table 1 Experimental conditions

Condition	Gap, h (mm)	Thermal gradient, T_Δ (°C/mm)
Free surface	Na	3.6, 5.0
Plate/plate	1.3, 1.5	3.6, 5.0
Sphere/plate	1.3, 1.4, 1.5	3.6, 5.0

Polydimethylsiloxane is a typical type of silicone oils and has excellent thermal stability and anti-volatility characteristics; here, this kind of silicone oil with a viscosity of 100 mPa·s was employed for the migration tests. In real working conditions, the contact surfaces were always impregnated with liquid lubricants. To mimic, all plates and spheres were wetted by the silicone oil before experiments. Moreover, the temperature on rubbing surfaces would rise to ~150 °C or higher under extreme working conditions such as high speed or contact pressure [17]; thus thermal gradients tested in this study were chosen accordingly. When the set temperature stabilized, 10 μL silicone oil droplets were injected to the surface or interfaces via a microsyringe. A digital camera (Canon, Japan) at top and a microscope (Keyence, Japan) at front were employed to monitor the whole migration process. As illustrated in Fig. 1, silicone oil maintains a spherical cap shape at the free surface, while it forms a liquid bridge at the plate/plate and the sphere/plate interfaces. Via a video processing software, accurate migration distance and velocity under different conditions can be calculated. The experimental conditions are listed in Table 1.
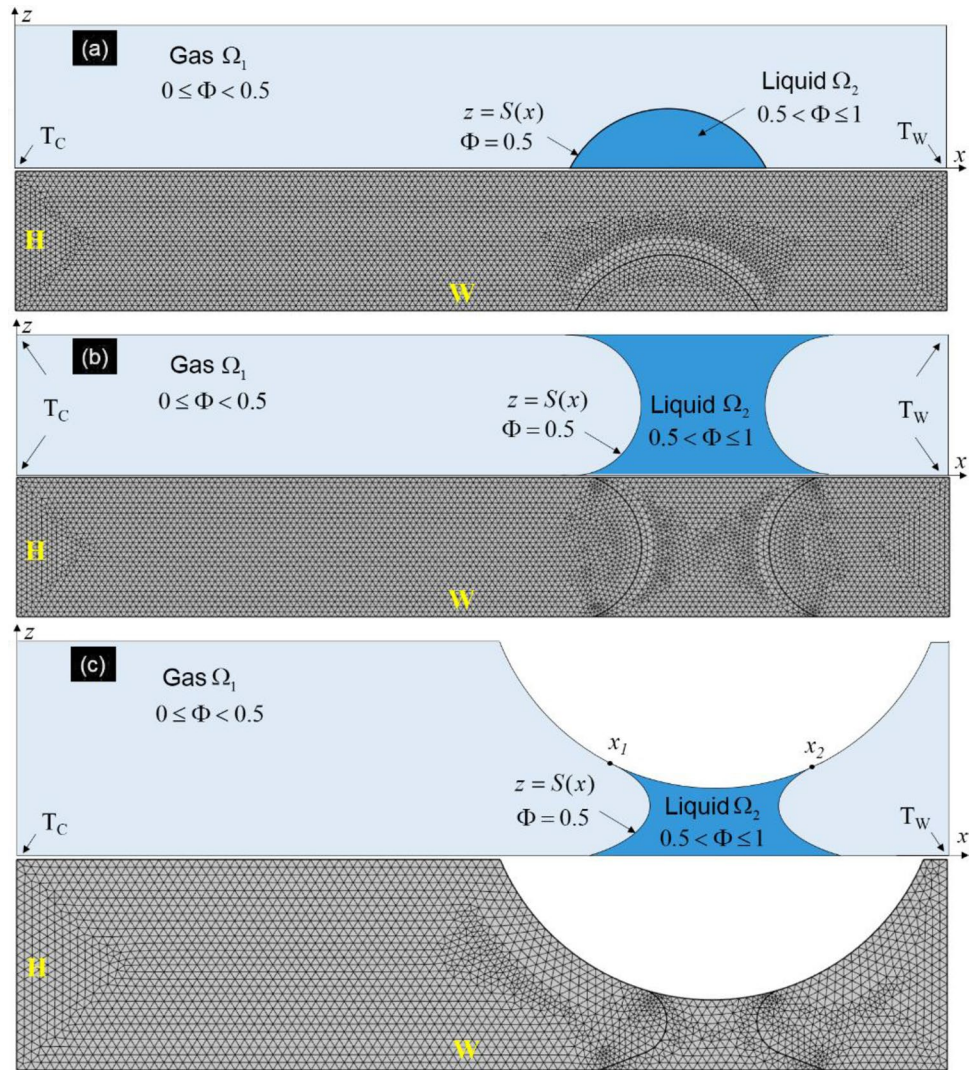
3 Simulations

3.1 Physical models

Previously, abundant investigations on the thermocapillary migration at free solid surfaces have proven that 2D (2-dimensional) numerical results are of high precision and reliability [18–24]. Here, a 2D simulation is performed at different interfaces to reveal the migration mechanism. As exhibited in Fig. 2, a droplet surrounded by gas is placed at a free surface in a rectangular computational domain with dimensions of 1.5×10 mm (height $H \times$ width W). Liquid bridges surrounded by gas are placed at the interfaces of plate/plate and sphere/plate, and the computational domains are 1.5×10 mm and 4.5×20 mm (height $H \times$ width W), respectively. The geometric dimensions of droplet and liquid bridges are obtained from the experimentally observed shapes. A constant thermal gradient T_Δ is applied on the bottom wall ($z = 0$) of the free surface and the sphere/plate interface, while on the bottom and top wall ($z = 0$ and $z = H$) of the plate/plate interface. Since the droplet dosage is relative small, its body force is neglected and the density is assumed to be constant. The fluids are assumed to be incompressible and Newtonian fluid.

The fluid flow interfaces are based on the Navier–Stokes equations, of which the continuity equation, conservation of momentum, and conservation of energy formulated in terms of temperature, can be expressed as:

Fig. 2 Schematic representations and meshes for computations of the migration under different conditions of the **a** free surface, **b** plate/plate interface, and **c** sphere/plate interface

$$\frac{\partial \rho}{\partial t} + \nabla \cdot (\rho \mathbf{U}) = 0 \qquad (1)$$

$$\rho \frac{\partial \mathbf{U}}{\partial t} + \rho(\mathbf{U} \cdot \nabla)\mathbf{U} = \nabla \cdot [-P\mathbf{I} + \tau] + \mathbf{F} \qquad (2)$$

$$\rho C_p \left(\frac{\partial T}{\partial t} + (\mathbf{U} \cdot \nabla)T \right) = -(\nabla \cdot \mathbf{q}) + \tau : \mathbf{R} - \frac{T}{\rho} \frac{\partial \rho}{\partial T}\Big|_P \left(\frac{\partial P}{\partial t} + (\mathbf{U} \cdot \nabla)P \right) + Q \qquad (3)$$

$$\rho C_p \frac{\partial T}{\partial t} + \rho C_p \mathbf{U} \cdot \nabla T + \nabla \cdot \mathbf{q} = Q$$
$$\mathbf{q} = -k\nabla T \qquad (4)$$

where k represents the fluid thermal conductivity.

In this study, the investigated thermocapillary migra-

where ρ represents the fluid density, U represents the velocity vector, P represents pressure, τ represents the viscous stress tensor, F represents the volume force vector, C_p represents the specific heat capacity at constant pressure, T represents the temperature, q represents the heat flux vector, Q represents the heat source, and R represents the strain-rate tensor: $\mathbf{R} = \frac{1}{2}(\nabla \mathbf{U} + (\nabla \mathbf{U})^T)$. To modeling the heat transfer in fluids, the following heat equation is employed:

tion belongs to Marangoni convection. Marangoni effect is a shear stress which depends on the tangential temperature gradient ($\nabla_t T$), and it has the following contribution described by forces induced at the liquid/gas interface:

$$[-p\mathbf{I} + \mu(\nabla \mathbf{U} + (\nabla \mathbf{U})^T) - \frac{2}{3}\mu(\nabla \cdot \mathbf{U})\mathbf{I}]\mathbf{n} = \gamma_T \nabla_t T \qquad (5)$$

where γ_T represents the surface tension coefficient of liquid. Assuming the surface tension (γ) of liquid varies linearly with temperature, this coefficient can be described as:

$$\gamma_T = \frac{\gamma(T) - \gamma(T_0)}{T - T_0} \tag{6}$$

The initial condition of velocity vector (U) is set as 0, and boundary conditions for these interfaces are defined as follows:

$$\text{Free surface:} \begin{cases} T(x, H) = T_{\text{ref}} \\ T(x, 0) = T_C + T_\Delta x \ ; \\ \text{Wetted wall at}(x, 0) \end{cases} \tag{7}$$

$$\text{Plate/plate:} \begin{cases} T(x, 0 \text{ or } H) = T_C + T_\Delta x \\ \text{Wetted wall at}(x, 0 \text{ or } H) \end{cases} ; \tag{8}$$

$$\text{Sphere/plate:} \begin{cases} T(x, z_{\max}) = T_{\text{ref}} \\ T(x, 0) = T_C + T_\Delta x \\ \text{Wetted wall at}(x, 0) \text{ and } (x_1 \le x \le x_2, z_{\max}) \end{cases} ; \tag{9}$$

where $T_{\text{ref}} = 20$ °C and $z_{\max}$ represents the maximum value of z at a specific x. All other walls are defined as nonslip walls, and the left and right walls are set as the insulation condition with a constant atmospheric pressure. Note that the upper wall of sphere/plate is different from that of plate/plate, physically, liquid lubricant cannot migrate uphill along the curved surface of sphere, the wetted zone between the liquid and the sphere is limited at the zone where the lubricant is injected. The nonslip wall boundary condition is a wall where the relative velocity between the fluid and the wall is zero. When the relative velocity is not zero, the wetted wall boundary condition is employed via initializing the parameters of contact angle (θ) and slip length (β) [19–22]. Moreover, for these cases, the gas/liquid interface of $S(x)$ (Fig. 2) must satisfy the kinematics condition and the continuity of the temperature, namely

$$U_l \nabla S = U_g \nabla S, \ T_l = T_g \tag{10}$$

where the subscripts l and g denotes liquid and gas, respectively.

3.2 Numerical Approach

The numerical simulations for migration have to account the movement and deforming of the interface. Various computational techniques have been developed that meet the requirements [19–22], of which the conservative level set method is a feasible candidate. The conservative level set method is a conceptual framework using level sets as a tool to model the incompressible two phase flow with the surface tension. One can perform numerical computations involving curves and surfaces on a fixed Cartesian grid without having to parameterize these objects [25, 26]. The whole computational domain Ω is divided into a gas subdomain Ω_1 ($0 \le \Phi < 0.5$) and a liquid subdomain Ω_2 ($0.5 < \Phi \le 1$), and the liquid/gas interface is located at $\Phi = 0.5$(Fig. 2). As the level set function Φ goes smoothly from 0 and 1, the fluids characteristics transform from gas phase to liquid phase correspondingly. The convection can be reinitialized as a function of Φ, that is:

$$\frac{\partial \Phi}{\partial t} + \mathbf{U} \cdot \nabla \Phi = \kappa \nabla \cdot \left[\varepsilon \nabla \Phi - \Phi(1 - \Phi) \frac{\nabla \Phi}{|\nabla \Phi|} \right] \tag{11}$$

where ε represents the interface thickness, κ represents the re-initialization parameter.

All the above-mentioned governing equations with the correlative boundary and initial conditions are solved via a segregated method (solving each physical field sequentially until converging) within a time-dependent solver developed by the COMSOL MULTIPHYSICS software. Different numbers of grids had been examined to achieve reliable results with sufficient accuracy and less computational time. Here, the maximum number of iterations is set to 10 for each time step, and the error in each integration step is controlled by the relative tolerance (A_{rt}) and absolute tolerance ($A_{at,k}$) for degrees of freedom (DOF) k, respectively. Setting $A_{rt} = 0.005$ and $A_{at,k} = 0.05$, and the step is accepted when:

$$\left(\frac{1}{M} \sum_j \frac{1}{N_j} \sum_k \left(\frac{|E_k|}{A_{at,k} + A_{rt}|V_k|} \right)^2 \right)^{1/2} < 1 \tag{12}$$

where M is the number of physical fields, N_j is the number of degrees of freedom (DOF) in field j, V_k is the solution vector corresponding to the solution at a specific time step k, E_k

Table 2 Physical properties of the liquids

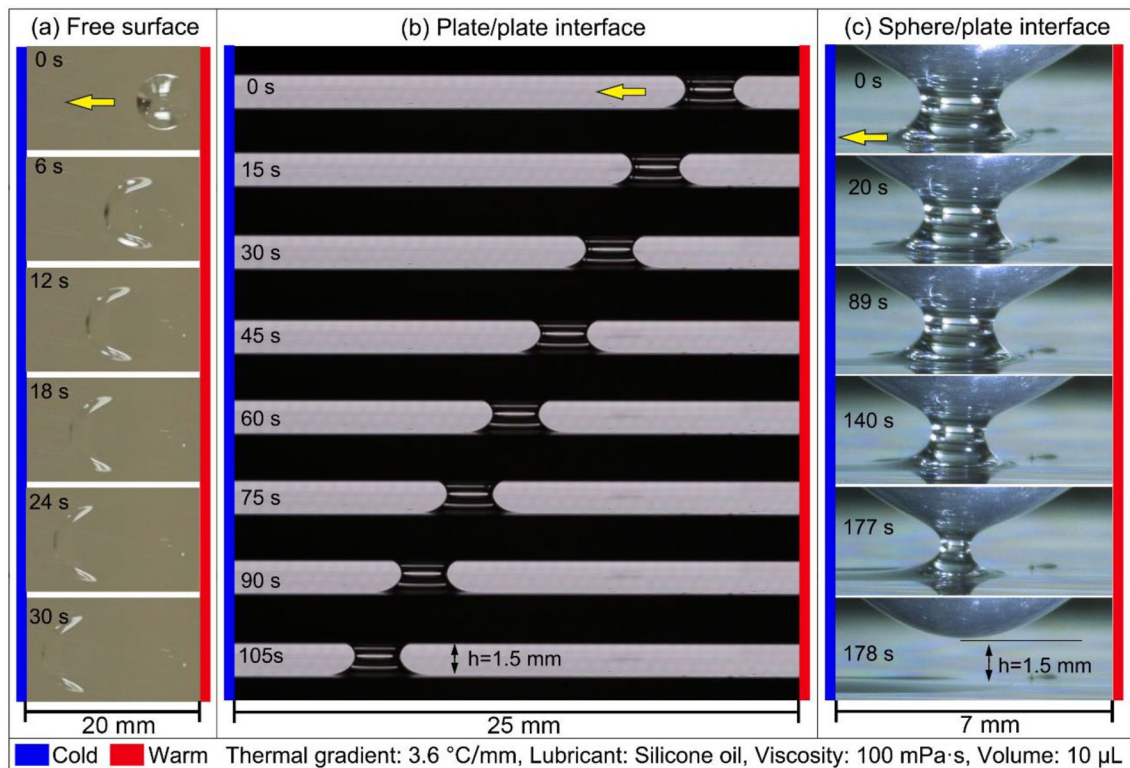| Parameters	Symbol	Value
Specific heat	C_p	1670 J/kg·K
Thermal conductivity	k	0.1 W/m·K
Thermal diffusivity	a	0.0618 mm²/s
Contact angle	θ	10°
Surface tension	γ	21 mN/m
Surface tension coefficient	γ_T	− 0.04 mN/m·K
Dynamic viscosity	μ	100 mPa·s
Liquid density	ρ	963 kg/m³

Fig. 3 Typical migration phenomena of silicone oils at the (a) free surface, (b) plate/plate, and (c) sphere/plate interfaces under a thermal gradient of 3.6 °C/mm

is the error estimate of the solver in V_k. Referring to Fig. 2, the DOFs in the computational domain for the free surface, the plate/plate interface, and the sphere/plate interface are 80,468, 50,737, 27,354, respectively. The physical properties of the liquid are listed in Table 2.

4 Results and Discussion

4.1 Experimental Results

Figure 3 shows the typical migration phenomena of silicone oils at the free surface, plate/plate and sphere/plate interfaces under a thermal gradient of 3.6 °C/mm. As shown in Fig. 3a, liquid lubricant migrates from the warm to the cold regions rapidly at the free surface over a migration distance of approximately 18 mm within 30 s. At the plate/plate interface, the formed liquid bridge also migrates to the cold side, while the required time for a distance of 18 mm is approximately 100 s, which is much longer than that of the free surface, as shown in Fig. 3b. An entirely different phenomenon is observed at the sphere/plate interface. As shown in Fig. 3c, the formed liquid bridge mainly maintains there, which is accompanied with a continuous loss of thin film toward the cold side on the plate. It takes ~170 s until

the liquid bridge breaks, and this breaking time is adopted for comparison. Moreover, compared with Fig. 3b and 3c, it is interesting to see that as the migration progresses, the liquid bridge is symmetrical at the plate/plate interface, while asymmetrical at the sphere/plate interface.

Figure 4 shows the detailed results for lubricants migration under different conditions. The influences of thermal gradient, gap between the plate/plate and the sphere/plate are investigated. Generally, a larger thermal gradient yields a faster migration velocity. As shown in Fig. 4a, the initial migration velocity at the free surface is approximately 2.3 mm/s under a thermal gradient of 5.0 °C/mm, and it decreases gradually as time elapses. Note that the viscosity of liquid decreases with increasing temperature, and liquids are more prone to migrate on a warmer surface [16]. As the migration progresses, the temperature of liquid and surface decreases correspondingly; thus the viscous dissipation would impede the thermal flow to some extent. As shown in Fig. 4b, the migration velocity at the plate/plate interface is much slower than that at the free surface under a same thermal gradient, and the migration behavior is weakened as the gap decreasing from 1.5 to 1.3 mm. Figure 4c exhibits the migration results at the sphere/plate interface, and it can be seen that the breaking time strongly depends on the gap (h), which decreases with increasing gap. The breaking time is
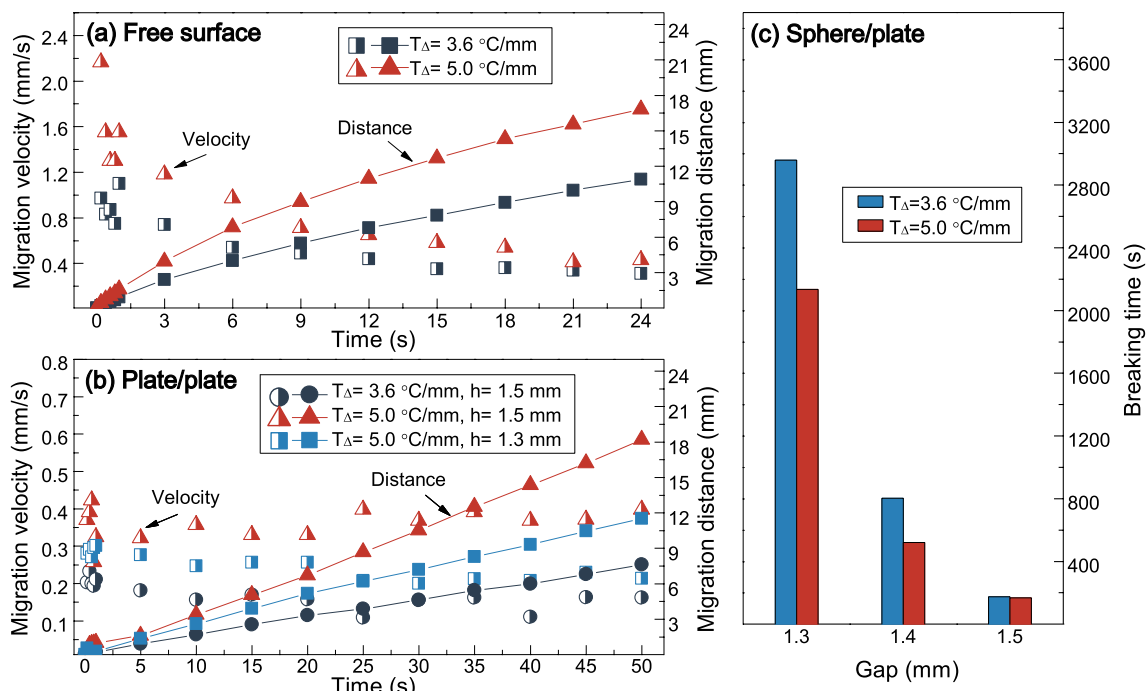
Fig. 4 Results for liquid lubricants migration under different conditions of **a** free surface, **b** plate/plate interface, and **c** sphere/plate interface

approximately 3000 s for a gap (*h*) of 1.3 mm, and it is only 160 s for a gap of 1.5 mm.

Referring to the above experimental results, it is confirmed that under the same thermal gradient, significant differences exist among the migration capacities of the free surface, the plate/plate interface, and the sphere/plate interface. These observed phenomena are quite interesting, while limited by the experimental observations, it is unknown what happens inside the liquid and how the differences originate. The internal mechanism and differences need to be further clarified.

4.2 Numerical Results

4.2.1 Numerical Phenomena

Figure 5 exhibits the numerical results of the volume fraction of the migrated liquid lubricants (silicone oil, viscosity of 100 mPa·s) at different interfaces subjected to a thermal gradient of 5 °C/mm. As shown in Fig. 5a, b, liquid lubricants migrate rapidly from the warm to the cold sides at the free surface and the plate/plate interface. At the sphere/plate interface, most lubricant adheres there and accompanying with a thin film migrating to the cold region, as shown in Fig. 5c. In general, the numerical results well simulate the observed experimental phenomena. Due to the limited dimensions of computational domains, the numerical and experimental velocities for the first second are compared and shown in Fig. 5d. Note that the numerical results are higher in magnitude compared to the experimental velocities. Nevertheless, the overall trends of the velocities are consistent, which increases rapidly to the maximum in the initial and then slows down gradually. The results are reliable to some extent, and the existing differences mainly originate from the following factors. First, all spheres and plates are naturally rough, the involved pinning effect [7] and contact angle hysteresis effect [15, 27] would obstruct the migration, and these effects are ignored in the numerical simulation. Second, ignoring the viscosity-temperature effect [28] in the numerical simulation would make the thermal convections inside the liquid more significant, yielding a higher calculated velocity. Moreover, the initial experimental stage of the migration process is complex, as a droplet placed onto the solid surface, the experimental time required for the droplet to reach the surface temperature is much higher than the numerical one. Besides, a 2D model would also make some errors, and it is expectable that a 3D model would achieve a more accurate results, which consumes a large amount of computational time.

Actually, Marangoni number describes the thermocapillary convection intensity of liquids, which can be expressed as: $Ma = \gamma_T T_\Delta d / \mu a$, where *d* represents the mean liquid thickness, *a* represents the fluid thermal diffusivity. A larger *Ma* number represents a more significant thermocapillary
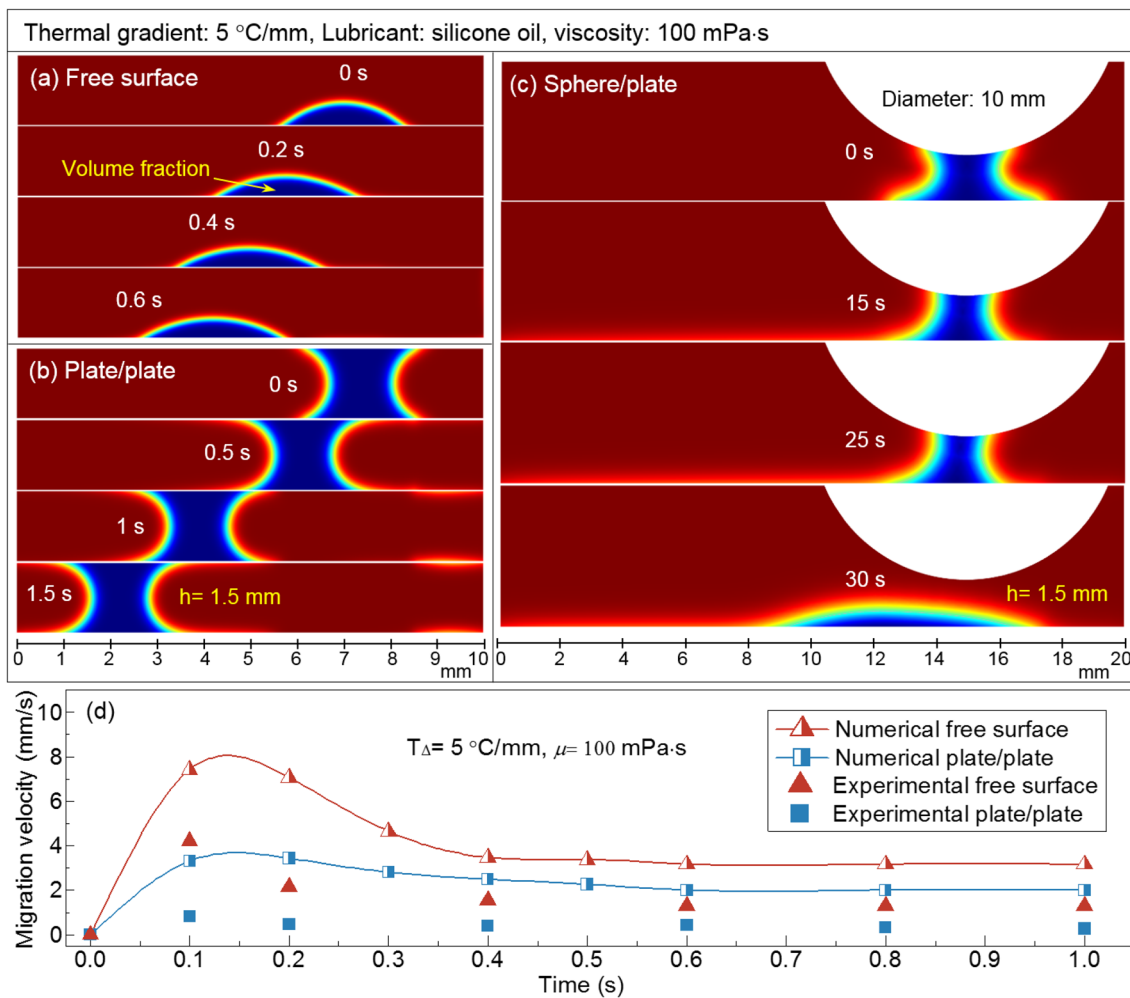
Fig. 5 Numerical results of volume fraction of the migrated liquid lubricants at the **a** free surface, **b** plate/plate interface, and **c** sphere/plate interface; **d** comparisons between the numerical and experimental results

convection intensity. Since the initial conditions for these conditions are the same and little difference exists among the values of Ma (~ 70) under different conditions, there should be other reasons for the differences. Hereby, the detailed temperature and flow fields inside the liquids are compared.

4.2.2 Temperature and Flow Fields Inside Liquids

Figure 6a shows the variation in the temperature fields at the free surface, and the difference between adjacent isotherms is 1 K. When the thermal gradient is activated, heat continues transmitting from the bottom wall to the liquid and gas. Since the thermal diffusion coefficient of liquid is much higher than that of gas, heat transmits faster inside the droplet. The obtained temperature distribution in Fig. 6a exhibits that at $t = 0.05$ s, an asymmetric thermal vortex is

formed inside the droplet. As the time increases to 0.2 s, the thermal vortex becomes smaller due to the gradual stability of temperature distribution. The corresponding flow field is shown in Fig. 6b, and it can be seen that thermocapillary convections are generated at the sharp regions of the formed thermal vortex. The convections are asymmetric at the warm and the cold sides, and a clear flow vortex is observed inside the droplet. Moreover, the entire convections are toward the cold side. These convections together activate the migration.

Figure 7 shows the variations in the temperature and flow fields inside the liquid bridge at the plate/plate interface over the elapsed time. Different from the free surface, the gradient is applied to both the upper and the lower plates. Consequently, the asymmetric thermal vortex is enlarged by the heat transmitted from the upper plate. As exhibits in Fig. 7a, a huge rectangular-like thermal vortex is formed inside the
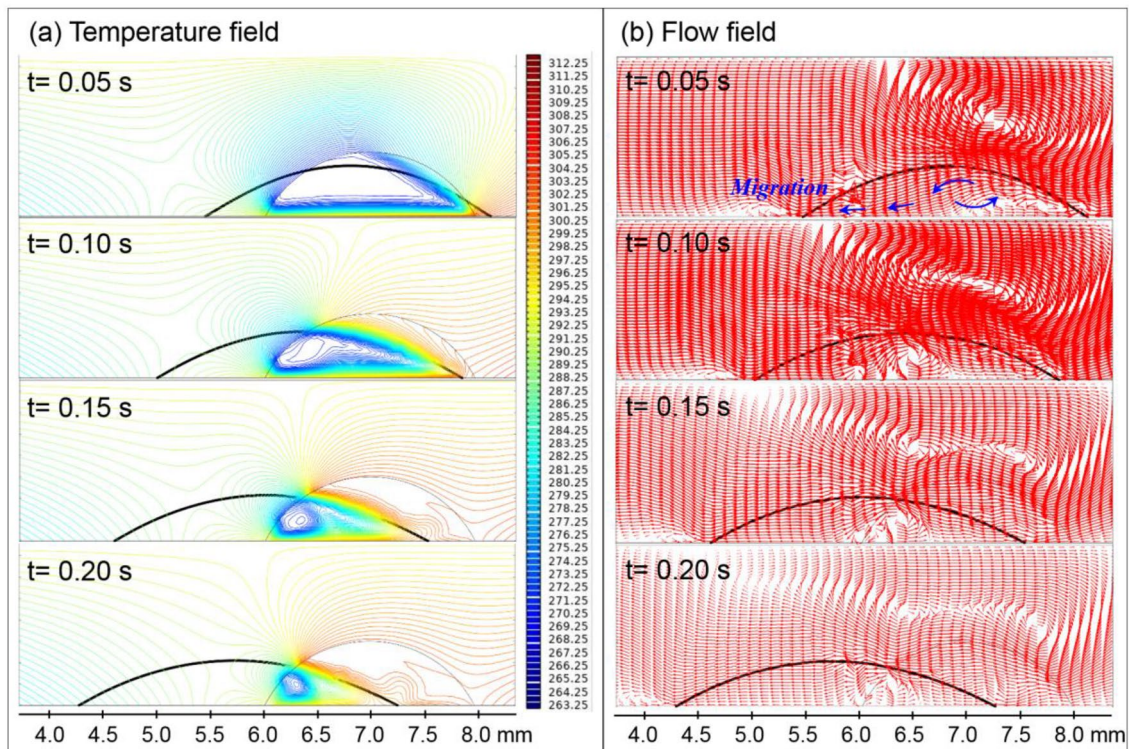
Fig. 6 Variations in the **a** temperature and **b** flow fields at the free surface over the elapsed time

liquid bridge ($t=0.05$ s), and this rectangular-like thermal vortex gradually dwindles as the time increases. It is noticed that temperature differences are significant at the vertexes of the thermal vortex, and four thermocapillary convections are formed there, as shown in Fig. 7b. The direction of the flow fields at the waist of the liquid bridge is from the warm to the cold sides. Accompanied by these inner convections, the overall flow fields are toward the cold side, contributing to the migration.

Figure 8a shows the variations in the temperature fields inside the liquid bridge at the sphere/plate interface over the elapsed time. The isotherms are deformed due to existence of the sphere, which forms a concave temperature distribution inside the liquid bridge. Four thermocapillary convections are generated at the vertexes of the liquid bridge and, moreover, the direction of the flow fields inside the liquid bridge is from the bottom to the top, as exhibited in Fig. 8b. Note that the intensities of the formed thermocapillary convections are in the same order of magnitude as the one shown in Fig. 7. However, due to the upward streams and the strong adhesion effect at the interface of sphere and liquid, the upper two convections have limited effects on the flow of the liquid bridge, and the liquid bridge can hardly migrate

integrally. In this case, only the convection at the cold side of the bottom wall can yield a movement.

4.3 Further Discussion

The flow fields can be further verified by the nepho-gram of the calculated values of the capillary numbers ($Ca = \mu U/\rho$) of these cases, as shown in Fig. S1 (in the supplementary material). With the numerical results of temperature and flow fields, migration mechanism at different interfaces can be understood. Since the surface tension of liquid decreases with increasing temperature, the formed thermal vortex could yield an unbalanced surface tension distribution. The well-known Marangoni effect [2] has proven that a liquid could move from a low-surface tension region to high one. Therefore, the thermal vortex can yield a thermocapillary convection inside the liquid. Among these three conditions, the thermocapillary convection of the free surface is most significant, which yields a fastest migration velocity. Through the comparison between Figs. 6a and 7a, it can be seen that the temperature difference in the liquid bridge at the plate/plate interface is significantly weaken by the heated upper plate.
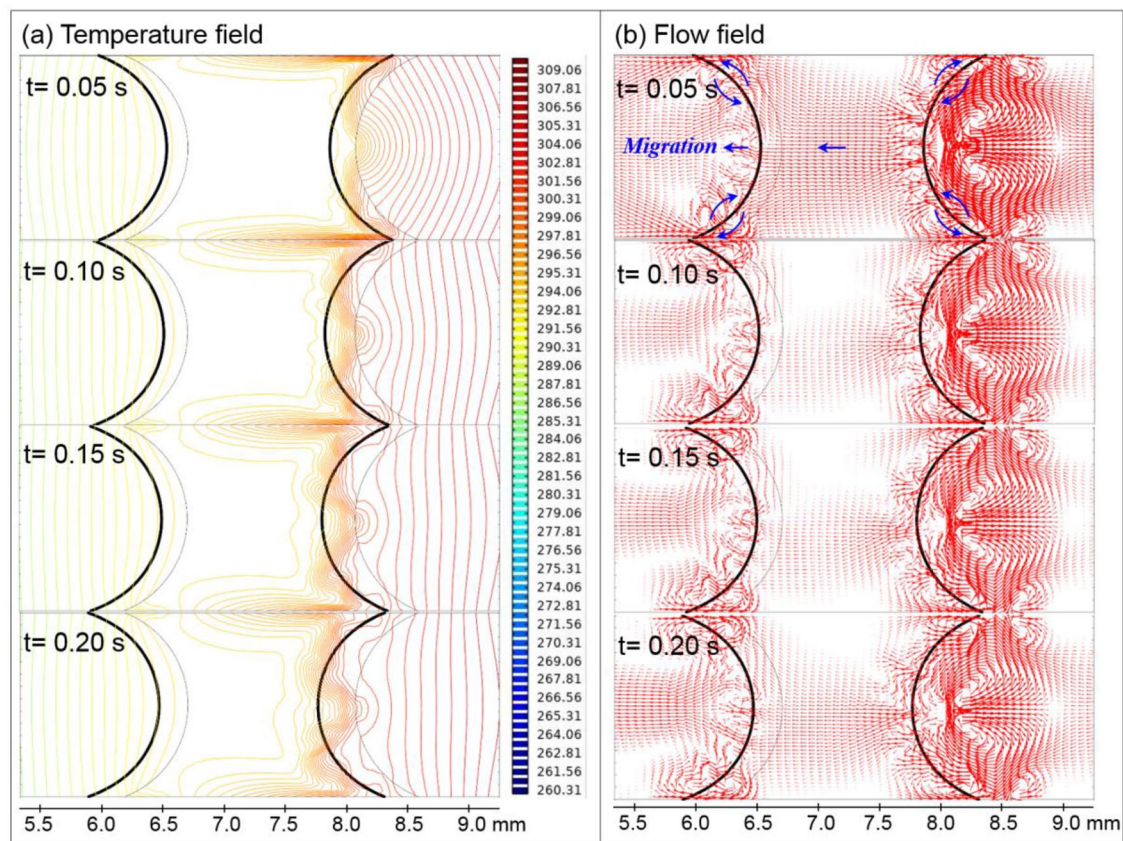
Fig. 7 Variations in the **a** temperature and **b** flow fields at the plate/plate interface over the elapsed time

Although four internal thermocapillary convections are generated inside the liquid bridge, the flow intensity is much weaker than that of the free surface, which yields a lower migration velocity. For the sphere/plate situation (Fig. 8), attributing to the independent sphere, migration phenomenon at the sphere/plate interface is different from the others. The curving sphere surface makes it difficult for liquids to move from the warm to the cold regions. More importantly, the inside upward streams and the strong adhesion effect between the sphere and liquid impedes the breaking of liquid bridge. Under the interaction effects, most liquid maintains at the interface, only the convection at the cold side of the bottom wall yields a slight migration.

5 Conclusion

In this study, the thermocapillary migration of liquid lubricants at the free surface, the plate/plate interface, and the sphere/plate interface is investigated experimentally and

numerically. It is confirmed that migration do occur under these conditions. Liquid lubricant can easily migrate at the free surface and the plate/plate interface, while it maintains at the sphere/plate interface for some time and a continuous loss of an extreme thin liquid film is observed at the cold side on the plate. Since the surface tension of liquid decreases with increasing temperature, the applied thermal gradients can form thermal vortexes inside liquids and generate thermocapillary convections, contributing to the migration. This study advances the understanding of interfacial phenomena and provides a general guidance for tribological interfaces that are exposed to thermal gradients. Generally, the migration behavior could be weaken by decreasing the thermal gradient or the gap between the interfaces. For the plate/plate interface, since thermocapillary convections mainly exist at the four vertexes of the liquid bridge, to obstruct the migration, specially attentions should be paid to these regions. For the sphere/plate interface, maintaining the temperature of the spheres at a relatively low level, enhancing the adhesion effect between the sphere and the lubricant, can impede the movement effectively.
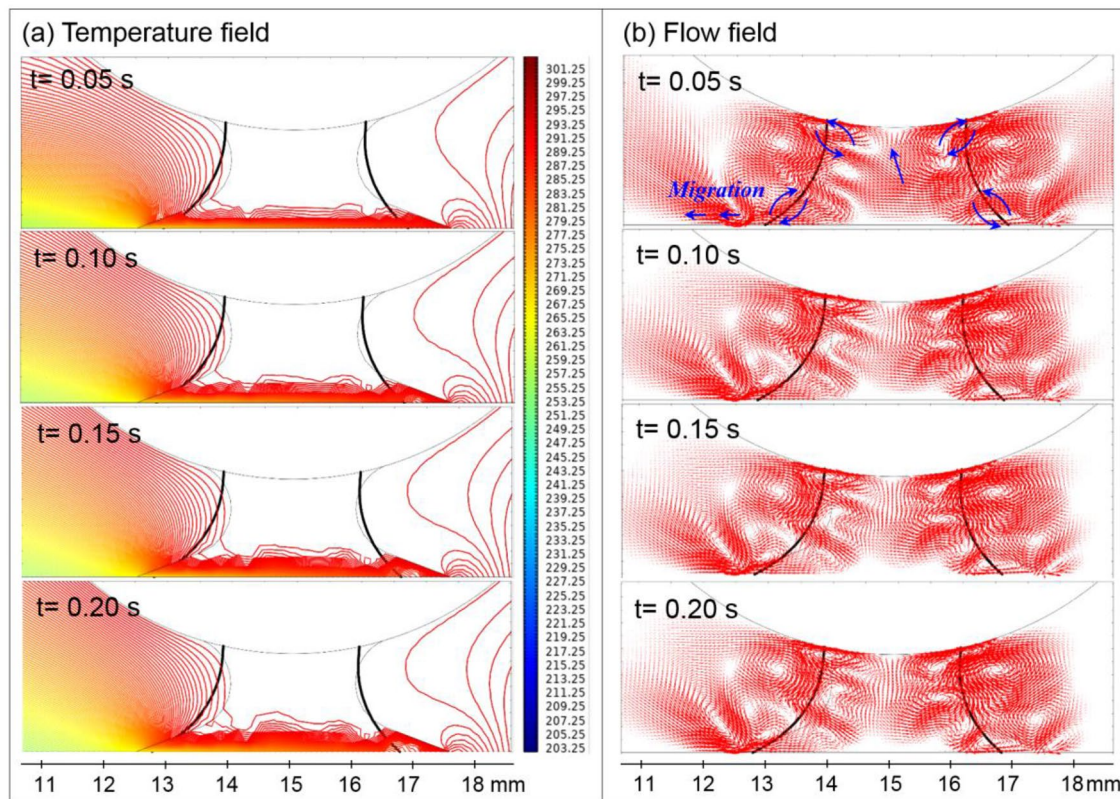
Fig. 8 Variations in the **a** temperature and **b** flow fields inside the liquid bridge at the sphere/plate interface over the elapsed time

References

1. Xu, X.F., Luo, J.B.: Marangoni flow in an evaporating water droplet. Appl. Phys. Lett. **91**(12), 124102 (2007)
2. Tadmor, R.: Marangoni flow revisited. J. Colloid Interface Sci. **332**(2), 451–454 (2009)
3. Scriven, L.E., Sternling, C.V.: The marangoni effects. Nature **187**, 186–188 (1960)
4. Jones, W.R., Jansen, M.J.: Tribology for space applications. Proc. Inst. Mech. Eng. Part J. J. Eng. Tribol. **222**(8), 997–1004 (2008)
5. Fote, A.A., Slade, R.A., Feuerstein, S.: The prevention of lubricant migration in spacecraft. Wear **51**(1), 67–75 (1978)
6. Dai, Q.W., Huang, W., Wang, X.L.: Surface roughness and orientation effects on the thermo-capillary migration of a droplet of paraffin oil. Exp. Therm. Fluid Sci. **57**, 200–206 (2014)
7. Dai, Q.W., Li, M., Khonsari, M.M., Huang, W., Wang, X.L.: The thermocapillary migration on rough surfaces. Lubr. Sci. **31**, 163–170 (2019)
8. Grützmacher, P.G., Rosenkranz, A., Szurdak, A., Gachot, C., Hirt, G., Mücklich, F.: Lubricant migration on stainless steel induced by bio-inspired multi-scale surface patterns. Mater. Des. **150**, 55–63 (2018)
9. Sommers, A.D., Brest, T.J., Eid, K.F.: Topography-based surface tension gradients to facilitate water droplet movement on laser-etched copper substrates. Langmuir **29**(38), 12043–12050 (2013)
10. Galatola, P.: Spontaneous capillary propulsion of liquid droplets on substrates with nonuniform curvature. Phys. Rev. Fluids **3**(10), 103601 (2018)
11. Dai, Q.W., Ji, Y.J., Chong, Z.J., Huang, W., Wang, X.L.: Manipulating thermocapillary migration via superoleophobic surfaces with wedge shaped superoleophilic grooves. J. Colloid Interface Sci. **557**, 837–844 (2019)
12. Brochard, F.: Motions of droplets on solid surfaces induced by chemical or thermal gradients. Langmuir **5**(2), 432–438 (1989)
13. Brzoska, J.B., Brochard-Wyart, F., Rondelez, F.: Motions of droplets on hydrophobic model surfaces induced by thermal gradients. Langmuir **9**(8), 2220–2224 (1993)
14. Ford, M.L., Nadim, A.: Thermocapillary migration of an attached drop on a solid surface. Phys. Fluids **6**(9), 3183–3185 (1994)
15. Chen, J.Z., Troian, S.M., Darhuber, A.A., Wagner, S.: Effect of contact angle hysteresis on thermocapillary droplet actuation. J. Appl. Phys. **97**(1), 014906 (2005)
16. Dai, Q.W., Huang, W., Wang, X.L., Khonsari, M.M.: Ringlike migration of a droplet propelled by an omnidirectional thermal gradient. Langmuir **34**(13), 3806–3812 (2018)
17. Khonsari, M.M., Booser, E.R.: Applied Tribology: Bearing Design and Lubrication. Wiley, Chichester (2008)
18. Wu, Z.B.: Terminal states of thermocapillary migration of a planar droplet at moderate and large marangoni numbers. Int. J. Heat Mass. Tran. **105**, 704–711 (2017)

19. Tseng, Y.-T., Tseng, F.-G., Chen, Y.-F., Chieng, C.-C.: Fundamental studies on micro-droplet movement by marangoni and capillary effects. Sens. Actuator A Phys. **114**(2–3), 292–301 (2004)

20. Nguyen, H.-B., Chen, J.-C.: A numerical study of thermocapillary migration of a small liquid droplet on a horizontal solid surface. Phys. Fluids **22**(6), 062102 (2010)

21. Le, T.-L., Chen, J.-C., Shen, B.-C., Hwu, F.-S., Nguyen, H.-B.: Numerical investigation of the thermocapillary actuation behavior of a droplet in a microchannel. Int. J. Heat Mass. Trans. **83**(Supplement C), 721–730 (2015)

22. Le, T.-L., Chen, J.-C., Nguyen, H.-B.: Numerical study of the thermocapillary droplet migration in a microchannel under a blocking effect from the heated upper wall. Appl. Therm. Eng. **122**, 820–830 (2017)

23. Liu, H., Wu, L., Ba, Y., Xi, G.: A lattice boltzmann method for axisymmetric thermocapillary flows. Int. J. Heat Mass. Trans. **104**, 337–350 (2017)

24. Liu, H., Zhang, Y.: Modelling thermocapillary migration of a microfluidic droplet on a solid surface. J. Comput. Phys. **280**, 37–53 (2015)

25. Olsson, E., Kreiss, G.: A conservative level set method for two phase flow. J. Comput. Phys. **210**(1), 225–246 (2005)

26. Olsson, E., Kreiss, G., Zahedi, S.: A conservative level set method for two phase flow ii. J. Comput. Phys. **225**(1), 785–807 (2007)

27. Dai, Q.W., Huang, W., Wang, X.L.: Contact angle hysteresis effect on the thermocapillary migration of liquid droplets. J. Colloid Interface Sci. **515**, 32–38 (2018)

28. Dai, Q.W., Khonsari, M.M., Shen, C., Huang, W., Wang, X.L.: Thermocapillary migration of liquid droplets induced by a unidirectional thermal gradient. Langmuir **32**(30), 7485–7492 (2016)